

Adaptive Block Sparse Regularization under Arbitrary Linear Transform

Takanobu Furuhashi
Nagoya Institute of Technology
Aichi, Japan
clz14116@nitech.jp

Hidekata Hontani
Nagoya Institute of Technology
Aichi, Japan
hontani.hidekata@nitech.ac.jp

Tatsuya Yokota
Nagoya Institute of Technology
Aichi, Japan
RIKEN Center for Advanced Intelligence Project
Tokyo, Japan
t.yokota@nitech.ac.jp

Abstract—We propose a convex and fast signal reconstruction method for block sparsity under arbitrary linear transform with unknown block structure. The proposed method is a generalization of the similar existing method and can reconstruct signals with block sparsity under non-invertible transforms, unlike the existing method. Our work broadens the scope of block sparse regularization, enabling more versatile and powerful applications across various signal processing domains. We derive an iterative algorithm for solving proposed method and provide conditions for its convergence to the optimal solution. Numerical experiments demonstrate the effectiveness of the proposed method.

Index Terms—Block-sparsity, non-invertible transform, TV regularization, signal recovery

I. INTRODUCTION

Many natural signals exhibit block sparsity. Block sparsity is a generalization of sparsity that evaluates the sparsity of signal components grouped by block structure. It has been shown to be more efficient than using mere sparsity in signal reconstruction [1], [2] and is applied in various signal processing and machine learning tasks [3]–[6]. Signal recovery based on block sparsity is performed using optimization with an appropriate observation matrix and block structure.

It is generally difficult to know the block structure in advance [7], so we consider optimizing while adaptively estimating the block structure. As shown in Table I, several methods have been proposed for this purpose [8]–[13]. We focus on Latent Optimally Partitioned ℓ_2/ℓ_1 (LOP- ℓ_2/ℓ_1), which is superior in both computational efficiency and convexity, and propose a method based on it. Since non-convex optimization problems have local minima, it is difficult to eliminate the influence of the initial value given to the algorithm. On the other hand, LOP- ℓ_2/ℓ_1 is convex and does not depend on the initial value. Furthermore, LOP- ℓ_2/ℓ_1 is computationally efficient and can be applied to large-scale problems.

However, LOP- ℓ_2/ℓ_1 cannot generally handle block sparsity of a feature vector under non-invertible transforms, as shown in Table II and Section II-B. For example, LOP- ℓ_2/ℓ_1 can handle block sparsity under invertible transforms such as Fourier transform. But LOP- ℓ_2/ℓ_1 cannot handle block sparsity for

This work was supported in part by the Japan Society for the Promotion of Science (JSPS) KAKENHI under Grant 23H03419 and Grant 20H04249.

¹Depends on the freedom of the assumed block structure.

²See (1) for variable J .

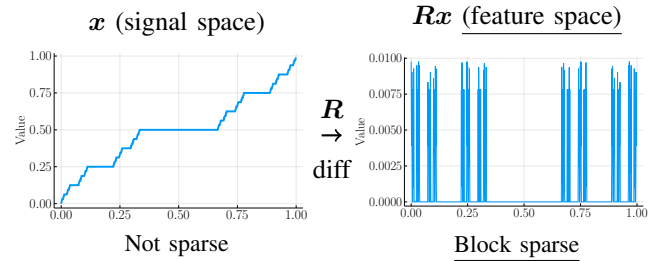


Fig. 1: Illustration of block sparsity under non-invertible transform (here, differentiation) in Cantor function [14].

differences of feature which is used in TV regularization [15], [16]. TV regularization is a typical approach that introduces a specific linear transformation to existing sparse regularization. On the other hand, in recent years, low-rank regularization under linear transform has been actively researched. In [17], low-rank tensor decomposition in the delayed embedded space has been proposed. In [18], [19] tensor nuclear norm regularization under framelet transformation has been proposed. In [20], low-rank matrix completion under arbitrary linear transformations has been proposed. This study can be said to be an analogy of these approaches, aiming at adaptive block sparse regularization under linear transformation.

To address this, we propose a novel method called Latent

TABLE I: Comparison of convexity and computational time of existing methods for block sparse regularization when the block structure is unknown.

Method	Convexity	Computational time
Greedy algorithm [8]	✗	$O(N^3)$
Bayesian methods [9], [10]	✗	$O(N^3)$
Latent Group Lasso [11], [12]	✓	Maximum $O(N^3)$ ¹
LOP- ℓ_2/ℓ_1 [13]	✓	$O(JN)$ ²

TABLE II: Comparison of the application range of existing and proposed methods in terms of the invertibility of linear transform R (see (5)).

R	LOP- ℓ_2/ℓ_1 ALT	LOP- ℓ_2/ℓ_1
invertible	✓	✓
non-invertible	✓	✗

Optimally Partitioned ℓ_2/ℓ_1 under Arbitrary Linear Transform (LOP- ℓ_2/ℓ_1 ALT) regularization, which can evaluate a more general form of block sparsity. Furthermore, we provide conditions for the convergence of the iterative algorithm for solving the proposed method to the optimal solution. To demonstrate the effectiveness of the proposed method, we apply it to artificial data and to ion current data obtained using nanopore technology.

II. PRELIMINARIES

A. Estimation of Unknown Block Sparsity

Let $\mathbf{y} = \mathbf{L}\mathbf{x} + \boldsymbol{\epsilon} \in \mathbb{C}^J$ be the observed vector, $\mathbf{L} \in \mathbb{C}^{J \times N}$ be the observation matrix, and $\boldsymbol{\epsilon} \in \mathbb{C}^J$ be the observation error. Block sparse regularization is performed by adding constraints to the solution of the optimization problem so that the estimated vector $\hat{\mathbf{x}} \in \mathbb{C}^N$ or its feature vector $\mathbf{R}\hat{\mathbf{x}} \in \mathbb{C}^K$ becomes block sparse, where $\mathbf{R} \in \mathbb{C}^{K \times N}$ is an arbitrary linear transform. The optimization problem that estimates the vector \mathbf{x} while constraining the solution using the LOP- ℓ_2/ℓ_1 penalty (2) is given as follows:

$$\min_{\mathbf{x} \in \mathbb{C}^N} f(\mathbf{L}\mathbf{x}) + \lambda \Psi_\alpha(\mathbf{x}), \quad (1)$$

where $\lambda \in \mathbb{R}_+$ is a regularization coefficient, $f: \mathbb{C}^J \rightarrow \mathbb{R}$ is a loss function that encourages $\mathbf{y} = \mathbf{L}\mathbf{x} + \boldsymbol{\epsilon}$ to be satisfied, and its proximal operator can be calculated efficiently. Such functions include squared error $f(\mathbf{L}\mathbf{x}) = \frac{1}{2} \|\mathbf{y} - \mathbf{L}\mathbf{x}\|_2^2$ and absolute error $f(\mathbf{L}\mathbf{x}) = \|\mathbf{y} - \mathbf{L}\mathbf{x}\|_1$.

LOP- ℓ_2/ℓ_1 [13] is a method that performs block-sparse regularization while estimating the unknown block structure using the LOP- ℓ_2/ℓ_1 penalty defined as follows:

$$\Psi_\alpha(\mathbf{x}) := \min_{\substack{\boldsymbol{\sigma} \in \mathbb{R}^N \\ \|\mathbf{D}\boldsymbol{\sigma}\|_1 \leq \alpha}} \varphi(\mathbf{x}, \boldsymbol{\sigma}), \quad (2)$$

(2) takes small value if \mathbf{x} has a block sparse structure with non-overlapping continuous blocks, which is enforced by the inequality constraint $\|\mathbf{D}\boldsymbol{\sigma}\|_1 \leq \alpha$ in (2). In addition, (2) is a convex function [13, Theorem 1] and (1) is a convex optimization problem if f is a convex function such as squared error or absolute error. $\boldsymbol{\sigma} \in \mathbb{R}^N$ represents latent vectors that indicate the estimated block structure. In other words, each element σ_n of $\boldsymbol{\sigma}$ corresponds to the block that element x_n of \mathbf{x} belongs to. $\alpha \in \mathbb{R}_+$ is a hyperparameter representing the upper limit of the estimated number of blocks. (2) converges to the ℓ_2 norm when $\alpha \rightarrow 0$ and to the ℓ_1 norm when $\alpha \rightarrow \infty$. $\mathbf{D} \in \mathbb{R}^{(N-1) \times N}$ is a differential operator for 1D signals represented as follows:

$$\mathbf{D} = \begin{bmatrix} -1 & 1 & 0 & \dots & 0 \\ 0 & \dots & \dots & \dots & \dots \\ \vdots & \dots & \dots & \dots & \dots \\ 0 & \dots & \dots & -0 & -1 & 1 \end{bmatrix},$$

and LOP- ℓ_2/ℓ_1 can be applied to high-dimensional signals such as images and videos by changing this operator according to

the dimension of the signal [13]. The function $\varphi: \mathbb{C}^N \times \mathbb{R}^N \rightarrow \mathbb{R}$ is defined as:

$$\varphi(\mathbf{x}, \boldsymbol{\sigma}) := \sum_{n=1}^N \phi(x_n, \sigma_n),$$

where the function $\phi: \mathbb{C} \times \mathbb{R} \rightarrow \mathbb{R}_+ \cup \{\infty\}$ is written as:

$$\phi(x, \tau) := \begin{cases} \frac{|x|^2}{2\tau} + \frac{\tau}{2}, & \text{if } \tau > 0; \\ 0, & \text{if } x = 0 \text{ and } \tau = 0; \\ \infty, & \text{otherwise.} \end{cases}$$

B. Limitations of the existing method

If \mathbf{R} is an invertible matrix, i.e., $(\mathbf{R}^\top \mathbf{R})^{-1}$ exists, (1) can be rewritten as follows:

$$\min_{\mathbf{x} \in \mathbb{C}^N} f(\mathbf{L}(\mathbf{R}^\top \mathbf{R})^{-1} \mathbf{R}^\top \mathbf{R}\mathbf{x}) + \lambda \Psi_\alpha(\mathbf{R}\mathbf{x}). \quad (3)$$

Then, let $\mathbf{z} = \mathbf{R}\mathbf{x} \in \mathbb{C}^K$ and $\tilde{\mathbf{L}} = \mathbf{L}(\mathbf{R}^\top \mathbf{R})^{-1} \mathbf{R}^\top \in \mathbb{C}^{J \times N}$, and (3) can be rewritten as follows:

$$\min_{\mathbf{z} \in \mathbb{C}^K} f(\tilde{\mathbf{L}}\mathbf{z}) + \lambda \Psi_\alpha(\mathbf{z}). \quad (4)$$

LOP- ℓ_2/ℓ_1 can be applied to (4) because it has the same form as (1). On the other hand, if \mathbf{R} is a non-invertible matrix, (1) cannot be rewritten in the form of (4), and LOP- ℓ_2/ℓ_1 cannot be applied.

III. PROPOSED METHOD

The proposed LOP- ℓ_2/ℓ_1 ALT method enables block structure estimation and regularization under various types of linear transforms. The optimization problem using LOP- ℓ_2/ℓ_1 ALT penalty is given as:

$$\min_{\mathbf{x} \in \mathbb{C}^N} f(\mathbf{L}\mathbf{x}) + \lambda \Psi_\alpha(\mathbf{R}\mathbf{x}). \quad (5)$$

Note that the input of Ψ_α is not \mathbf{x} but a feature vector $\mathbf{R}\mathbf{x}$. When $\mathbf{R} = \mathbf{I}$, (5) is equivalent to (1), then the proposed method is an extension of LOP- ℓ_2/ℓ_1 . By substituting (2), we can rewrite (5) as:

$$\min_{(\mathbf{x}, \boldsymbol{\sigma}) \in \mathbb{C}^N \times \mathbb{R}^K} f(\mathbf{L}\mathbf{x}) + \lambda \varphi(\mathbf{R}\mathbf{x}, \boldsymbol{\sigma}), \quad \text{s.t. } \|\mathbf{D}\boldsymbol{\sigma}\|_1 \leq \alpha. \quad (6)$$

Further, we apply the equality constraints $\mathbf{u} = \mathbf{L}\mathbf{x}$, $\mathbf{v} = \mathbf{R}\mathbf{x}$, $\boldsymbol{\eta} = \mathbf{D}\boldsymbol{\sigma}$ to (6) and replace the inequality constraint $\|\mathbf{D}\boldsymbol{\sigma}\|_1 \leq \alpha$ with the indicator function of the ℓ_1 -norm ball:

$$\iota_{B_1^\alpha}(\boldsymbol{\eta}) := \begin{cases} 0, & \text{if } \|\boldsymbol{\eta}\|_1 \leq \alpha; \\ \infty, & \text{otherwise.} \end{cases}$$

This yields the following expression for (7):

$$\min_{\substack{(\mathbf{x}, \boldsymbol{\sigma}) \in \mathbb{C}^N \times \mathbb{R}^K \\ (\mathbf{u}, \mathbf{v}, \boldsymbol{\eta}) \in \mathbb{C}^J \times \mathbb{C}^K \times \mathbb{R}^{K-1}}} \underbrace{f(\mathbf{u}) + \lambda \varphi(\mathbf{v}, \boldsymbol{\sigma}) + \iota_{B_1^\alpha}(\boldsymbol{\eta})}_{=G(\mathbf{w})}, \quad \text{s.t. } \underbrace{\begin{bmatrix} \mu_1 \mathbf{L} & \mathbf{O} & -\mu_1 \mathbf{I} & \mathbf{O} & \mathbf{O} \\ \mu_2 \mathbf{R} & \mathbf{O} & \mathbf{O} & -\mu_2 \mathbf{I} & \mathbf{O} \\ \mathbf{O} & \mu_3 \mathbf{D} & \mathbf{O} & \mathbf{O} & -\mu_3 \mathbf{I} \end{bmatrix}}_{=\mathbf{H}} \underbrace{\begin{bmatrix} \mathbf{x} \\ \boldsymbol{\sigma} \\ \mathbf{u} \\ \mathbf{v} \\ \boldsymbol{\eta} \end{bmatrix}}_{=\mathbf{w}} = \mathbf{0}. \quad (7)$$

Algorithm 1 Loris-Verhoeven iteration [21]

Input: $\tau_1, \tau_2 > 0, \mathbf{w}^0 \in \mathbb{C}^{N'}, \mathbf{r}^0 \in \mathbb{C}^{J'}$ **Output:** $\mathbf{w} \in \mathbb{C}^{N'}$ **for** $i = 0, 1, 2, \dots$ **do**
 $\tilde{\mathbf{w}}^{i+1} = \mathbf{w}^i + \tau_1 \mathbf{H}^* (\mathbf{r}^i - \tau_2 \mathbf{H} \mathbf{w}^i)$
 $\mathbf{w}^{i+1} = \text{prox}_{\tau_1 G}(\tilde{\mathbf{w}}^{i+1})$
 $\mathbf{r}^{i+1} = \mathbf{r}^i - \tau_2 \mathbf{H} \mathbf{w}^{i+1}$

Algorithm 2 Solver for LOP- ℓ_2/ℓ_1 ALT (5)

Input: $\tau_1, \tau_2, \mu_1, \mu_2, \mu_3 > 0, \mathbf{x}^0 \in \mathbb{C}^N, \boldsymbol{\sigma}^0 \in \mathbb{R}^K, \mathbf{u}^0 \in \mathbb{C}^J, \mathbf{v}^0 \in \mathbb{C}^K, \boldsymbol{\eta}^0 \in \mathbb{R}^{K-1}, \mathbf{r}_1^0 \in \mathbb{C}^J, \mathbf{r}_2^0 \in \mathbb{C}^K, \mathbf{r}_3^0 \in \mathbb{R}^{K-1}, \Delta \mathbf{r}_1^0 \in \mathbb{C}^J, \Delta \mathbf{r}_2^0 \in \mathbb{C}^K, \Delta \mathbf{r}_3^0 \in \mathbb{R}^{K-1}$ **Output:** $\mathbf{x} \in \mathbb{C}^N, \boldsymbol{\sigma} \in \mathbb{R}^K,$ **for** $i = 0, 1, 2, \dots$ **do**
 $\tilde{\mathbf{x}}^{i+1} = \mathbf{x}^i + \tau_1 \mu_1 \mathbf{L}^* (\mathbf{r}_1^i - \tau_2 \Delta \mathbf{r}_1^i) + \tau_1 \mu_2 \mathbf{R}^* (\mathbf{r}_2^i - \tau_2 \Delta \mathbf{r}_2^i)$
 $\tilde{\boldsymbol{\sigma}}^{i+1} = \boldsymbol{\sigma}^i + \tau_1 \mu_3 \mathbf{D}^\top (\mathbf{r}_3^i - \tau_2 \Delta \mathbf{r}_3^i)$
 $\tilde{\mathbf{u}}^{i+1} = \mathbf{u}^i + \tau_1 \mu_1 (\mathbf{r}_1^i - \tau_2 \Delta \mathbf{r}_1^i)$
 $\tilde{\mathbf{v}}^{i+1} = \mathbf{v}^i + \tau_1 \mu_2 (\mathbf{r}_2^i - \tau_2 \Delta \mathbf{r}_2^i)$
 $\tilde{\boldsymbol{\eta}}^{i+1} = \boldsymbol{\eta}^i + \tau_1 \mu_3 (\mathbf{r}_3^i - \tau_2 \Delta \mathbf{r}_3^i)$
 $\mathbf{x}^{i+1} = \tilde{\mathbf{x}}^{i+1}$
 $\mathbf{u}^{i+1} = \text{prox}_{\tau_1 f}(\tilde{\mathbf{u}}^{i+1})$
 $(\mathbf{v}^{i+1}, \boldsymbol{\sigma}^{i+1}) = \text{prox}_{\tau_1 \lambda \varphi}(\tilde{\mathbf{v}}^{i+1}, \tilde{\boldsymbol{\sigma}}^{i+1})$
 $\boldsymbol{\eta}^{i+1} = \text{prox}_{\ell_{B_1^\alpha}}(\tilde{\boldsymbol{\eta}}^{i+1}) = P_{B_1^\alpha}(\tilde{\boldsymbol{\eta}}^{i+1})$ by (8)
 $\Delta \mathbf{r}_1^{i+1} = \mu_1 (\mathbf{L} \mathbf{x}^i - \mathbf{u}^i)$
 $\Delta \mathbf{r}_2^{i+1} = \mu_2 (\mathbf{R} \mathbf{x}^i - \mathbf{v}^i)$
 $\Delta \mathbf{r}_3^{i+1} = \mu_3 (\mathbf{D} \boldsymbol{\sigma}^i - \boldsymbol{\eta}^i)$
 $\mathbf{r}_1^{i+1} = \mathbf{r}_1^i - \tau_2 \Delta \mathbf{r}_1^{i+1}$
 $\mathbf{r}_2^{i+1} = \mathbf{r}_2^i - \tau_2 \Delta \mathbf{r}_2^{i+1}$
 $\mathbf{r}_3^{i+1} = \mathbf{r}_3^i - \tau_2 \Delta \mathbf{r}_3^{i+1}$

In this expression, $\mathbf{H} \in \mathbb{C}^{J' \times N'}, G : \mathbb{C}^{N'} \rightarrow \mathbb{R}$, and the problem can be formulated as:

$$\min_{\mathbf{w} \in \mathbb{C}^{N'}} G(\mathbf{w}) \text{ s.t. } \mathbf{H} \mathbf{w} = \mathbf{0}.$$

To solve this problem, we can use the Loris Verhoeven iteration, which is one of the primal-dual methods. The Loris Verhoeven iteration is described in Algorithm 1. By applying (7) to Algorithm 1, we obtain the optimization algorithm for LOP- ℓ_2/ℓ_1 ALT penalty, as shown in Algorithm 2. The symbols used in Algorithm 2 are explained as follows. The projection onto the ℓ_1 -norm ball with radius α is defined as:

$$P_{B_1^\alpha}(\boldsymbol{\eta}) := \begin{cases} \boldsymbol{\eta}, & \text{if } \|\boldsymbol{\eta}\|_1 \leq \alpha; \\ (a_k \text{sign}(\eta_k))_{k=1}^{K-1}, & \text{otherwise.} \end{cases} \quad (8)$$

where the coefficients a_k are defined as:

$$a_k := \max \left\{ \left| \eta_k \right| - \frac{1}{T} \left(\sum_{t=1}^T \rho_t - \alpha \right), 0 \right\},$$
$$T := \max \left\{ t \in \{1, \dots, K-1\} \left| \frac{1}{t} \left(\sum_{n=1}^t \rho_n - \alpha \right) < \rho_t \right. \right\},$$

and $\rho_1, \dots, \rho_{K-1}$ are sorted in descending order of $|\eta_1|, \dots, |\eta_{K-1}|$.

Additionally, we evaluated the conditions under which Algorithm 2 converges to the optimal solution. By performing this evaluation rigorously, we can obtain upper bounds for $\mu_1, \mu_2, \mu_3 > 0$, which can accelerate the convergence to the optimal solution of Algorithm 2. It is known that the Loris-Verhoeven iteration converges to the optimal solution when $\tau_1 \tau_2 \|\mathbf{H}\|_{\text{op}}^2 \leq 1$. By applying this condition to the proposed method, $\|\mathbf{H}\|_{\text{op}}$ can be calculated as follows:

$$\|\mathbf{H}\|_{\text{op}} = \sqrt{\rho(\mathbf{H}\mathbf{H}^*)}$$
$$= \sqrt{\rho \left(\begin{bmatrix} \mu_1^2(\mathbf{L}\mathbf{L}^* + \mathbf{I}) & \mu_1 \mu_2 \mathbf{L}\mathbf{R}^* & \mathbf{O} \\ \mu_1 \mu_2 \mathbf{R}\mathbf{L}^* & \mu_2^2(\mathbf{R}\mathbf{R}^* + \mathbf{I}) & \mathbf{O} \\ \mathbf{O} & \mathbf{O} & \mu_3^2(\mathbf{D}\mathbf{D}^\top + \mathbf{I}) \end{bmatrix} \right)},$$

where $\rho(\mathbf{A})$ is the maximum eigenvalue of \mathbf{A} . $\mathbf{H}\mathbf{H}^*$ can be rewritten as follows because it is a block diagonal matrix when considering the 2×2 and 1×1 block matrices separately:

$$\left\{ \rho \left(\begin{bmatrix} \mu_1^2(\mathbf{L}\mathbf{L}^* + \mathbf{I}) & \mu_1 \mu_2 \mathbf{L}\mathbf{R}^* \\ \mu_1 \mu_2 \mathbf{R}\mathbf{L}^* & \mu_2^2(\mathbf{R}\mathbf{R}^* + \mathbf{I}) \end{bmatrix} \right) \leq (\tau_1 \tau_2)^{-1} \right. \quad (9a)$$
$$\left. \mu_3^2 (\|\mathbf{D}\|_{\text{op}}^2 + 1) \leq (\tau_1 \tau_2)^{-1}. \right. \quad (9b)$$

(9b) gives an upper bound for μ_3 . On the other hand, it is difficult to explicitly solve (9a) for μ_1, μ_2 unless the left-hand side matrix is block diagonal, i.e., $\mathbf{L}\mathbf{R}^* = \mathbf{O}$, and it is not possible to give upper bounds for them. However, in the range of experiments we conducted, we were able to satisfy (9a) by setting μ_1, μ_2 as follows:

$$\begin{cases} 0 \leq \mu_1 \leq \frac{(\tau_1 \tau_2)^{-1/2}}{\sqrt{2\|\mathbf{L}\|_{\text{op}}^2 + 1}} \\ 0 \leq \mu_2 \leq \frac{(\tau_1 \tau_2)^{-1/2}}{\sqrt{2\|\mathbf{R}\|_{\text{op}}^2 + 1}} \end{cases}$$

Therefore, although we cannot give upper bounds for μ_1, μ_2 , we believe that this is not a problem in practice.

IV. NUMERICAL EXPERIMENTS

In this section, we demonstrate the effectiveness of the proposed method by comparing the results of denoising with TV regularization [15]. However, we do not compare it with LOP- ℓ_2/ℓ_1 because it cannot be applied to signals with block sparse derivatives. First, we verify the effectiveness of the proposed method on artificial data with block sparse derivatives. Additionally, we demonstrate that over-smoothing is less likely to occur for strong noise settings, as in TV regularization, by denoising actual ion currents.

Synthetic Examples: To investigate the performance of the proposed method, we performed denoising experiments on artificial data with block sparse derivatives. The artificial data was generated using the signal $\mathbf{x} \in \mathbb{R}^{1000}$ with the same block sparsity as Fig. 1 as follows: $\mathbf{y} = \mathbf{x} + \boldsymbol{\epsilon}$, where $\mathbf{y} \in \mathbb{R}^{1000}$ is the observed signal and $\boldsymbol{\epsilon} \in \mathbb{R}^{1000}$ is the white Gaussian noise. The loss function is the squared

TABLE III: Comparison of SNR of denoised signals of artificial data (Fig. 1) with noise added to obtain the specified SNR. The hyperparameters are set to the values that gave the best results for each SNR.

noise level (SNR)	LOP- ℓ_2/ℓ_1 ALT	TV
10	25.68	24.15
15	28.68	27.54
20	31.83	31.00
25	35.34	34.50
30	38.94	38.19

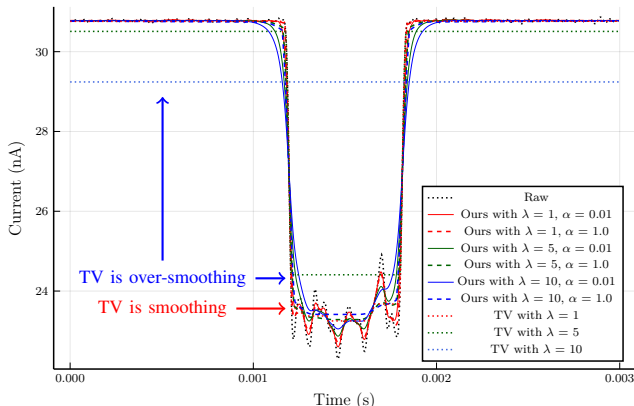


Fig. 2: Comparison of denoising results for ion currents. The red, green, and blue lines represent the estimated values for $\lambda = 1, 5, 10$, respectively.

error with a regularization term. The signal \mathbf{x} is estimated from the noisy observed signal \mathbf{y} under the above settings. The evaluation index of the denoising ability is the average SNR ($= 10 \log_{10} \|\mathbf{x}\|_2^2 / \|\mathbf{x} - \hat{\mathbf{x}}\|_2^2$) of the estimated signals $\hat{\mathbf{x}}$ obtained by performing the estimation independently 20 times. The SNR of the signals estimated by the proposed method and TV regularization is shown in Table III. The proposed method shows better SNR than TV regularization, indicating that it is superior in denoising.

Application to ion current data: To demonstrate the robustness of the proposed method to over-smoothing, we perform denoising experiments on ion currents. The noisy observed signal $\mathbf{y} \in \mathbb{R}^{750}$ is estimated from the signal $\mathbf{x} \in \mathbb{R}^{750}$ under the same settings as in the artificial data experiment. The results of denoising are shown in Fig. 2, and the blocks estimated by the proposed method are shown in Fig. 3. From the results, it can be seen that the proposed method is less likely to be over-smoothed by large λ , in this case $\lambda \in \{5, 10\}$, compared to TV regularization. This can be seen from the fact that over-smoothing does not occur in the proposed method when $\alpha = 0.1$, which correctly estimates the block structure, compared to the other methods.

Application to natural image: We demonstrate the high denoising performance of the proposed method for removing salt-and-pepper noise in images and the effect of estimating block structure on the recovery results. The latter result allows

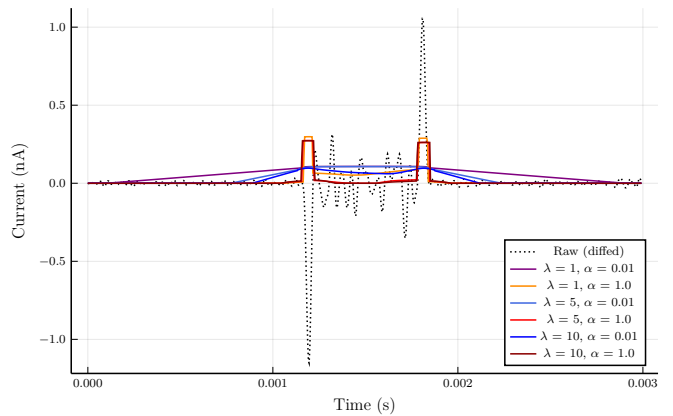


Fig. 3: Comparison of block structure of ion current derivatives estimated by the proposed method.

us to obtain a policy for selecting the regularization parameter λ of the proposed method based on the appropriate one in TV regularization. Since there are already many studies on selecting the appropriate parameter for TV regularization [22]–[24], we can reduce the risk of choosing the wrong one for the proposed method by using them. For this purpose, we compare the results of denoising a 256×256 image with the white Gaussian noise (Fig. 4, right in the first row) using TV regularization and the proposed method. The second row of Fig. 4 is a case where the smoothing by TV regularization is insufficient ($\lambda = 0.15$). In this case, it is clear that the proposed method improves denoising by estimating the block structure to suppress the salt-and-pepper noise. On the other hand, the third row of Fig. 4 is a case where TV regularization performs sufficient smoothing ($\lambda = 0.22$). In contrast to the previous case, the proposed method shows lower SNR than TV regularization and blurs the image. Therefore, it can be seen that the estimated block structure is hindering denoising.

From Fig. 4 results, it is expected that the regularization parameter λ of the proposed method should be set smaller than that for TV regularization to obtain sufficient denoising.

V. CONCLUSION

In this paper, we proposed LOP- ℓ_2/ℓ_1 ALT regularization and its optimization algorithm. We also derived the conditions under which the optimization algorithm converges to the optimal solution. The proposed method is a generalization of LOP- ℓ_2/ℓ_1 [13] based on non-invertible transform. Additionally, we performed denoising experiments using LOP- ℓ_2/ℓ_1 ALT regularization. The proposed method is less likely to be over-smoothed than TV regularization and is superior in denoising. As future work, it is necessary to analyze the convergence conditions of the proposed method more rigorously, demonstrate the effectiveness of block sparse regularization using non-derivative non-invertible transforms, and clarify the policy for selecting hyperparameters (λ, α) appropriately.

Acknowledgments: We thank Prof. Uemura and Mr. Akita

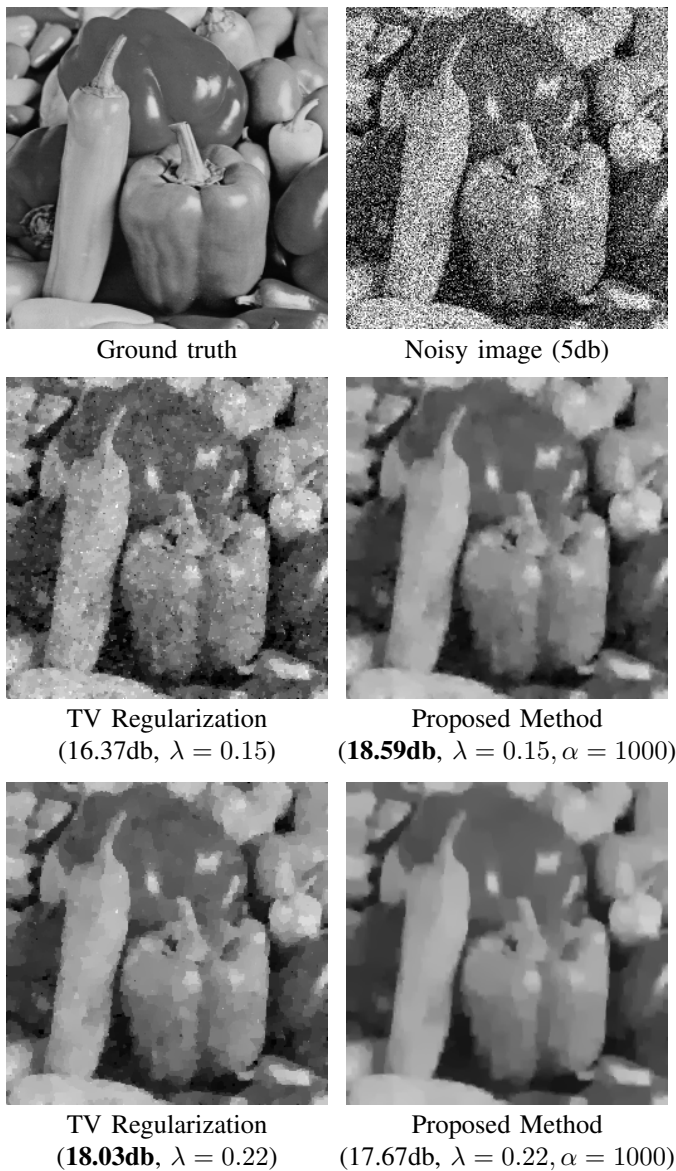


Fig. 4: Comparison of denoising results for natural images.

at the University of Tokyo for providing us with ion current data from the nanopore device.

REFERENCES

- [1] Richard G. Baraniuk, Volkan Cevher, Marco F. Duarte, and Chinmay Hegde, "Model-Based Compressive Sensing," *IEEE Transactions on Information Theory*, vol. 56, no. 4, pp. 1982–2001, Apr. 2010.
- [2] Yonina C. Eldar, Patrick Kuppinger, and Helmut Bolcskei, "Block-sparse signals: Uncertainty relations and efficient recovery," *IEEE Transactions on Signal Processing*, vol. 58, no. 6, pp. 3042–3054, 2010.
- [3] Guoshen Yu, StÉphane Mallat, and Emmanuel Bacry, "Audio Denoising by Time-Frequency Block Thresholding," *IEEE Transactions on Signal Processing*, vol. 56, no. 5, pp. 1830–1839, May 2008.
- [4] R. Gribonval and E. Bacry, "Harmonic decomposition of audio signals with matching pursuit," *IEEE Transactions on Signal Processing*, vol. 51, no. 1, pp. 101–111, Jan. 2003.
- [5] Lei Yu, Hong Sun, Jean Pierre Barbot, and Gang Zheng, "Bayesian Compressive Sensing for clustered sparse signals," in *2011 IEEE International Conference on Acoustics, Speech and Signal Processing (ICASSP)*, May 2011, pp. 3948–3951.
- [6] Nu Wen, Renzhong Guo, Biao He, Yong Fan, and Ding Ma, "Block-sparse CNN: Towards a fast and memory-efficient framework for convolutional neural networks," *Applied Intelligence*, vol. 51, no. 1, pp. 441–452, Jan. 2021.
- [7] Daichi Kitahara, Hiroki Kuroda, Akira Hirabayashi, Eiichi Yoshikawa, Hiroshi Kikuchi, and Tomoo Ushio, "Nonlinear Beamforming Based on Group-Sparsities of Periodograms for Phased Array Weather Radar," *IEEE Transactions on Geoscience and Remote Sensing*, vol. 60, pp. 1–19, 2022.
- [8] Junzhou Huang, Tong Zhang, and Dimitris Metaxas, "Learning with structured sparsity," in *Proceedings of the 26th Annual International Conference on Machine Learning*, Montreal Quebec Canada, June 2009, pp. 417–424, ACM.
- [9] Jun Fang, Yanning Shen, Hongbin Li, and Pu Wang, "Pattern-coupled sparse bayesian learning for recovery of block-sparse signals," *IEEE Transactions on Signal Processing*, vol. 63, no. 2, pp. 360–372, 2015.
- [10] Lu Wang, Lifan Zhao, Susanto Rahardja, and Guoan Bi, "Alternative to extended block sparse bayesian learning and its relation to pattern-coupled sparse bayesian learning," *IEEE Transactions on Signal Processing*, vol. 66, no. 10, pp. 2759–2771, May 2018.
- [11] Laurent Jacob, G. Obozinski, and Jean-Philippe Vert, "Group lasso with overlap and graph lasso," in *Proceedings of ICML '09*, 2009.
- [12] Guillaume Obozinski, Laurent Jacob, and Jean-Philippe Vert, "Group lasso with overlaps: The latent group lasso approach," Research report, Oct. 2011.
- [13] Hiroki Kuroda and Daichi Kitahara, "Block-sparse recovery with optimal block partition," *IEEE Transactions on Signal Processing*, vol. 70, pp. 1506–1520, 2022.
- [14] O. Dovgoshay, O. Martio, V. Ryazanov, and M. Vuorinen, "The Cantor function," *Expositiones Mathematicae*, vol. 24, no. 1, pp. 1–37, Feb. 2006.
- [15] Leonid I. Rudin, Stanley Osher, and Emad Fatemi, "Nonlinear total variation based noise removal algorithms," *Physica D: Nonlinear Phenomena*, vol. 60, no. 1, pp. 259–268, Nov. 1992.
- [16] Wei He, Hongyan Zhang, Liangpei Zhang, and Huanfeng Shen, "Total-Variation-Regularized Low-Rank Matrix Factorization for Hyperspectral Image Restoration," *IEEE Transactions on Geoscience and Remote Sensing*, vol. 54, no. 1, pp. 178–188, Jan. 2016.
- [17] Tatsuya Yokota, Burak Erem, Seyhmus Guler, Simon K. Warfield, and Hidekata Hontani, "Missing slice recovery for tensors using a low-rank model in embedded space," in *Proceedings of the IEEE Conference on Computer Vision and Pattern Recognition (CVPR)*, June 2018.
- [18] Jian-Li Wang, Ting-Zhu Huang, Xi-Le Zhao, Tai-Xiang Jiang, and Michael K. Ng, "Multi-Dimensional Visual Data Completion via Low-Rank Tensor Representation Under Coupled Transform," *IEEE Transactions on Image Processing*, vol. 30, pp. 3581–3596, 2021.
- [19] Tai-Xiang Jiang, Michael K. Ng, Xi-Le Zhao, and Ting-Zhu Huang, "Framelet Representation of Tensor Nuclear Norm for Third-Order Tensor Completion," *IEEE Transactions on Image Processing*, vol. 29, pp. 7233–7244, 2020.
- [20] Chao Li, Wei He, Longhao Yuan, Zhun Sun, and Qibin Zhao, "Guaranteed Matrix Completion Under Multiple Linear Transformations," in *2019 IEEE/CVF Conference on Computer Vision and Pattern Recognition (CVPR)*, Long Beach, CA, USA, June 2019, pp. 11128–11137, IEEE.
- [21] Ignace Loris and Caroline Verhoeven, "On a generalization of the iterative soft-thresholding algorithm for the case of non-separable penalty," *Inverse Problems*, vol. 27, no. 12, pp. 125007, Dec. 2011.
- [22] Manasavee Lohvithee, Ander Biguri, and Manuchehr Soleimani, "Parameter selection in limited data cone-beam CT reconstruction using edge-preserving total variation algorithms," *Physics in Medicine & Biology*, vol. 62, no. 24, pp. 9295–9321, Nov. 2017.
- [23] J. Mead and Department of Mathematics, Boise State University, Boise, ID, USA, "\$\chi^2\$ test for total variation regularization parameter selection," *Inverse Problems & Imaging*, vol. 14, no. 3, pp. 401–421, 2020.
- [24] Babak Maboudi Afkham, Julianne Chung, and Matthias Chung, "Learning regularization parameters of inverse problems via deep neural networks," *Inverse Problems*, vol. 37, no. 10, pp. 105017, Oct. 2021.